



OPEN ACCESS

EDITED BY

Lan Zhao, School of Medicine, Stanford University, United States

REVIEWED BY

Haitao Chen,
School of Public Health, Sun Yat-sen University, China
Anjali Lathwal,
Indraprastha Institute of Information Technology Delhi, India
Meng Zhou,
Wenzhou Medical University, China

*CORRESPONDENCE

Xiao-Liang Xing,
xiaoliangxinghnm@126.com

[†]These authors have contributed equally to this work

SPECIALTY SECTION

This article was submitted to Cancer Genetics and Oncogenomics, a section of the journal Frontiers in Genetics

RECEIVED 07 April 2022

ACCEPTED 06 July 2022

PUBLISHED 30 August 2022

CITATION

Han Z, Wang H, Liu Y and Xing X-L (2022), Establishment of a prognostic ferroptosis- and immune-related long noncoding RNAs profile in kidney renal clear cell carcinoma. *Front. Genet.* 13:915372. doi: 10.3389/fgene.2022.915372

COPYRIGHT

© 2022 Han, Wang, Liu and Xing. This is an open-access article distributed under the terms of the [Creative Commons Attribution License \(CC BY\)](https://creativecommons.org/licenses/by/4.0/). The use, distribution or reproduction in other forums is permitted, provided the original author(s) and the copyright owner(s) are credited and that the original publication in this journal is cited, in accordance with accepted academic practice. No use, distribution or reproduction is permitted which does not comply with these terms.

Establishment of a prognostic ferroptosis- and immune-related long noncoding RNAs profile in kidney renal clear cell carcinoma

Zhijun Han^{1,2†}, Hao Wang^{1,3†}, Yafei Liu¹ and Xiao-Liang Xing^{1,2*}

¹Department of Urology, Department of Ultrasonography, Zhuzhou Hospital Affiliated to Xiangya school of Medicine, Central South University, Zhuzhou, China, ²School of Public Health and Laboratory Medicine, Hunan University of Medicine, Huaihua, China, ³Department of Urology, The First Affiliated Hospital, Hengyang Medical School, University of South China, Huaihua, China

Background: Ferroptosis and immunity are novel treatments that target several cancers, including kidney renal clear cell carcinoma (KIRC). Long noncoding RNAs (lncRNAs) are an important class of gene expression regulators that play fundamental roles in the regulation of ferroptosis and immunity. We aimed to identify ferroptosis- and immune-related lncRNAs as biomarkers in patients with KIRC.

Methods: Corresponding data for each patient with KIRC were obtained from The Cancer Genome Atlas (TCGA) database. Univariate and multivariate Cox regression analyses were used to identify candidate biomarkers followed by least absolute shrinkage and selection operator (LASSO) regression analyses, weighted gene coexpression network analysis (WGCANA), and gene set enrichment analysis (GSEA).

Results: Three ferroptosis- and immune-related differentially expressed lncRNAs (FI-DEs) (AC124854.1, LINC02609, and ZNF503-AS2) were markedly and independently correlated with the overall survival (OS) of patients with KIRC. The area under the curve (AUC) value of the prognostic model in the entire group using the three FI-DEs was > 0.70. The sensitivity and specificity of the diagnostic model using the three FI-DEs were 0.8586 and 0.9583, respectively.

Conclusion: The present study found that AC124854.1, LINC02609, and ZNF503-AS2 were considerably and independently correlated with the OS of patients with KIRC, suggesting that the three FI-DEs could be used as prognostic and diagnostic biomarkers for patients with KIRC.

KEYWORDS

KIRC, ferroptosis, immune, lncRNAs, prognosis, diagnosis

1 Introduction

Kidney cancer is one of the most common malignant tumors originating in the kidneys. In 2020, approximately 180,000 deaths and 430,000 new cases of kidney cancer were reported globally (Sung et al., 2021). Almost 90% of kidney cancers are renal cell carcinoma (KIRC) (Singh, 2021). According to the morphology, renal cell carcinoma can be mainly divided into three subtypes: kidney renal clear cell carcinoma (KIRC), kidney renal papillary cell carcinoma, and kidney chromophobe (Owens, 2016). The most common subtype of kidney cancer is KIRC, and it accounts for approximately 80% of all primary malignant kidney tumors (Song et al., 2019; Zhou et al., 2020). Additionally, previous studies have demonstrated that 60% of patients with KIRC die within the first 2–3 years, and 30% of patients with KIRC are diagnosed with metastases (Mendoza-Alvarez et al., 2019). Moreover, numerous studies have demonstrated that the prognosis of patients with KIRC with metastases is poor (Chaffer and Weinberg, 2011; Forsea et al., 2012; Ljungberg et al., 2015). Currently, pathological tumors, nodes, and metastasis (TNM) are usually used as a biomarker to assess the risk of patients with KIRC (Wang et al., 2019a). Additionally, numerous studies have indicated that several molecular biomarkers, such as IL13RA2, SKI, and P4HB, can guide diagnosis, prognosis, and therapy (Salama et al., 2015; Shibasaki et al., 2015; Xie et al., 2020). However, the prognosis and diagnosis of KIRC remain poor. Therefore, it is necessary to obtain reliable biomarkers for the diagnosis and prognosis of patients with KIRC.

Ferroptosis is an iron-dependent form of cell death. Numerous studies have indicated that dysregulation of ferroptosis participates in the carcinogenesis and development of several cancers (Dixon et al., 2012; Nie et al., 2018). The regulation of ferroptosis contributes to anticancer therapy in various cancers, including drug-resistant cancers, such as non-small cell lung cancer and pancreatic cancer (Yamaguchi et al., 2013; Efferth, 2017). Immunotherapy targets specific cancer antigens and alerts the immune system to eradicate them through a concerted immune response (Johdi and Sukor, 2020). Immune cells and immune factors not only participate in antitumor immunity but also in the initiation and development of antitumor immunity (Berraondo et al., 2016; Chen et al., 2017). Cancer immunotherapy has been successfully used to treat many cancers (Im and Pavletic, 2017; Nixon et al., 2018). Interestingly, evidence indicates that there is a close link between ferroptosis and immunity. Ferroptosis cells can interact with immune cells such as NK cells and CD8+ T cells, among others, to release chemotaxis to regulate anticancer immunity (Wang et al., 2018a; Wang et al., 2019b; Stockwell and Jiang, 2019). Ferroptosis and immunity can regulate each other to participate in anticancer effects (Wang et al., 2019b; Stockwell and Jiang, 2019; Shi et al., 2021). The synergistic regulation of ferroptosis and immunity not only inhibits carcinogenesis but also stimulates immune responses (Li and Rong, 2020).

The lncRNAs are a group of transcriptional RNAs over 200 nucleotides in length that cannot encode proteins and are

TABLE 1 Characteristics of KIRC patients.

Characteristic	Variable	Total (n = 530)	%
Age (years)	≤ 65	348	65.66
	> 65	182	34.34
Gender	Female	186	35.09
	Male	344	64.91
Stage	Stage I	265	50.00
	Stage II	57	10.75
	Stage III	123	23.21
	Stage IV	82	15.47
	Unknown	3	0.57
Tumor classification	T1	271	51.13
	T2	69	13.02
	T3	179	33.77
	T4	11	2.08
Lymph nodes	N0	239	45.09
	N1	16	3.02
	Unknown	275	51.89
Distant metastasis	M0	422	79.62
	M1	78	14.72
	Unknown	30	5.66
Survival status	Alive	357	67.36
	Death	173	32.64

considered one of the most sensitive and specific cancer biomarkers (Fazal and Chang, 2016). Furthermore, they are involved in carcinogenesis and the development of various cancers (Wang et al., 2018b; Kim et al., 2018; Zhang et al., 2018; Slack and Chinnaiyan, 2019). Many lncRNAs can be used as prognostic biomarkers for several cancers, such as bladder cancer and lung cancer (Sun et al., 2020a; Zhang et al., 2021; Zhou et al., 2021). In this study, we evaluated FI-DEs as potential prognostic biomarkers using differential expression, Pearson correlation, and univariate/multivariate Cox regression analyses.

2 Materials and methods

2.1 Acquisition of corresponding data

The read counts data of KIRC (72 normal individuals and 530 patients with KIRC) and their corresponding clinical information (Table 1) were downloaded from an open database The Cancer Genome Atlas (TCGA) which do not need the approval of the local ethics committee. The read counts data of KIRC (45 normal individuals and 91 patients with KIRC) were downloaded from another open database International Cancer Genome Consortium (ICGC). DEseq2 in R (3.6.1) was used to screen the differentially expressed genes (DEGs) as the following criteria: $\text{baseMean} \geq 100$, $|\log_2\text{FoldChange}| \geq 1.00$, and $p_{\text{adj}} <$

0.05. The recognized lncRNAs, ferroptosis-related genes, and recognized immune-related genes were downloaded from the GENCODE database (<https://portal.gdc.cancer.gov/>), FerrDb database (<http://www.zhounan.org/ferrdb>), and ImmPort database (<http://www.immport.org>).

Estimate in R (3.6.1) was used to evaluate the stromal, immune, and ESTIMATE scores and tumor purity. The evaluated infiltrating score of immune cells and immune factors was downloaded from Tumor IMMune Estimation Resource (TIMER) (<https://cistrome.shinyapps.io/timer/>).

2.2 Acquisition of ferroptosis- and immune-related signatures

After differentially expressed analyses, overlapping analyses were carried out for the differentially expressed genes (DEGs) with the recognized ferroptosis- and immune-related genes to screen the ferroptosis- and immune-related DEGs (FI-DEGs) and with the recognized lncRNAs to screen the DELs. Pearson correlation analyses were performed for the FI-DEGs and DELs to obtain the FI-DELs as the following criteria $r \geq 0.5$ and $p < 0.05$.

2.3 Acquisition of prognostic biomarkers

The median value of each gene expression was used to regroup the patients with KIRC into low- and high-expression groups. Univariate Cox regression analyses followed by least absolute shrinkage and selection operator (LASSO) regression analyses were used to investigate the relationship of the FI-DELs with their overall survival (OS). Then, multivariate Cox regression analyses were performed to screen the suitable FI-DELs as biomarkers.

2.4 WGCNA and gene set enrichment analysis

The TIMER algorithm was utilized to estimate the stromal score, immune score, tumor purity, and ESTIMATE score. We used WGCNA that can convert coexpression correlation into connection weights, to identify coexpressed genes in stromal and immune cells (Langfelder and Horvath, 2008). Kyoto Encyclopedia of Genes and Genomes (KEGG) was used to assess the biological roles of the prognostic candidates by the “clusterProfiler” R package.

2.5 Construction of prognostic and diagnostic models

According to previous reports (Liu et al., 2020), the candidate biomarkers were used to construct a risk assessment model as

follows: risk value = $(0.831) \times \text{LINC02609 expression value} + (-0.585) \times \text{ZNF503-AS2 expression value} + (-0.530) \times \text{AC124854.1 expression value}$. A comprehensive index of ferroptosis and immune status (CIFI) was evaluated as follows: $\text{CIFI} = (\text{risk score} - \text{Min}) / \text{Max}$. The Youden index was used as the optimal cut-off value to regroup the patients with KIRC into low and high CIFI groups.

A diagnostic model was constructed as following after a stepwise logistic regression analyses: $\text{logit}(P) = 0.747 + (0.212) \times \text{LINC02609 expression value} + (-0.145) \times \text{ZNF503-AS2 expression value} + (0.200) \times \text{AC124854.1 expression value}$ (Liu et al., 2020). The Youden index was used as the optimal cut-off value to regroup the sample into a normal group and a KIRC group.

2.6 Statistical analyses

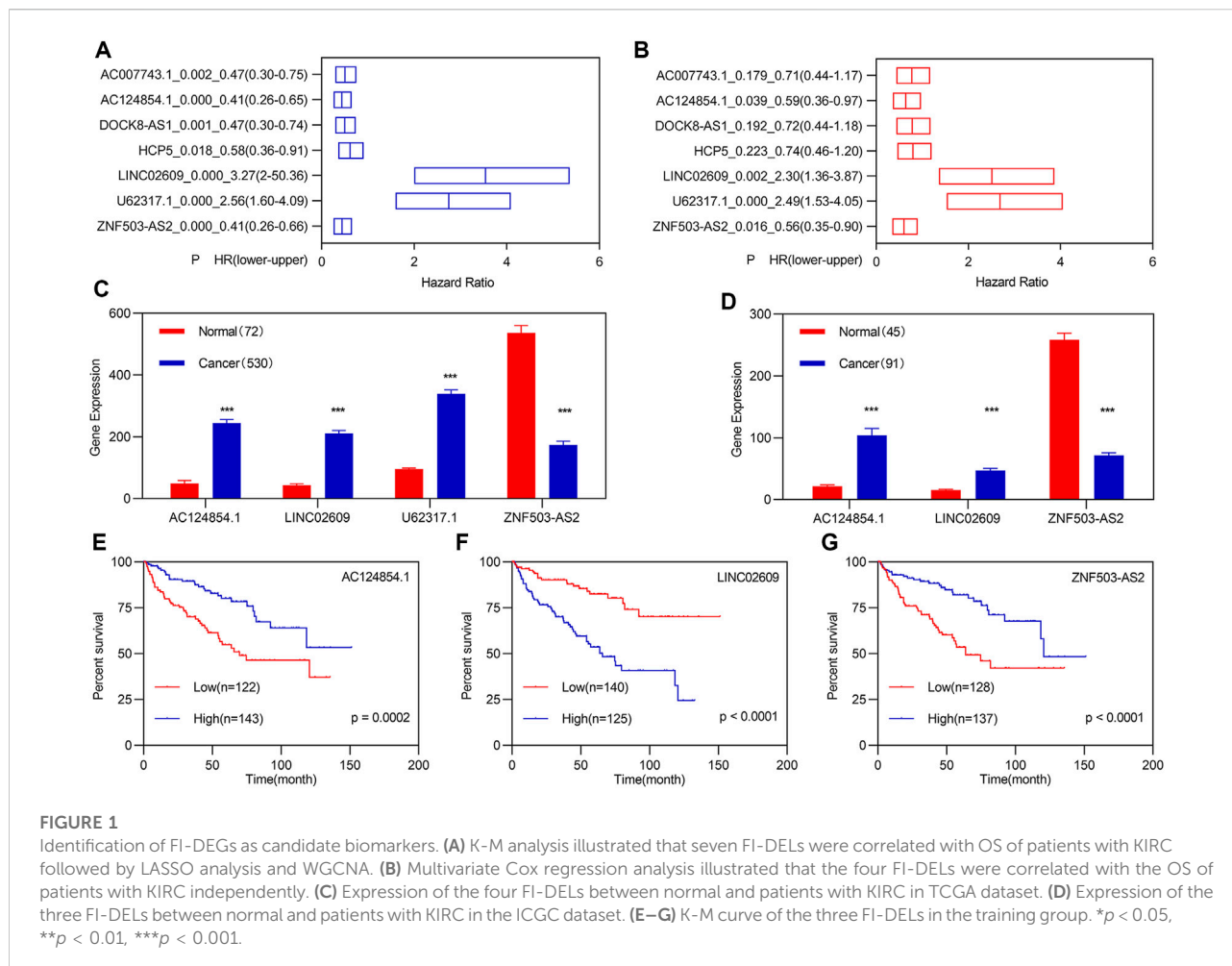
A repeated measure ANOVA followed by an unpaired two-tailed student's t-test was used as indicated. All results were expressed as the mean \pm SEM. Principal component analyses were used to reduce the dimensions and visualize the distribution of KIRC patients with different CIFI scores.

3 Results

3.1 Identification of ferroptosis- and immune-related differentially expressed lncRNAs as candidate biomarkers

Through differential expression analyses, we obtained 3,978 DEGs, including 2,573 upregulated and 1,405 downregulated DEGs (Supplementary Figure S1A). Of these, there were 531 FI-DEGs (405 upregulated FI-DEGs and 126 downregulated FI-DEGs) (Supplementary Figure S1B) and 361 DELs (278 upregulated DELs and 83 downregulated DELs) (Supplementary Figure S1C). Pearson correlation analyses for the 531 FI-DEGs and 361 DELs found that there were 3,483 FI-DEGs–DELs pairs involving 362 FI-DEGs and 261 DELs. These 261 DELs were renamed FI-DELs.

All patients with KIRC ($n = 530$) were randomly divided into training ($n = 265$) and validation ($n = 265$) groups to verify and obtain suitable biomarkers. Univariate Cox regression analyses followed by LASSO analyses for the 261 FI-DELs in the training group were performed, and results indicated that 17 FI-DELs were correlated with the OS of patients with KIRC (Supplementary Figure S1D–F). Through ESTIMATE analyses in R software (3.6.1), we found that the stromal, immune, and ESTIMATE scores were considerably increased, while tumor purity was markedly decreased in patients with KIRC (Supplementary Figure S2A–D). In the TCGA-KIRC cohort dataset, we obtained 38 modules using WGCNA (Figures



2E,F). Of which, six modules and seven models were highly correlated with stromal and immune scores, respectively, which enriched 2,858 lncRNAs. By overlapping analyses with the 17 FI-DEs, we obtained seven FI-DEs (Figure 1A). Next, multivariate Cox regression analyses for the seven FI-DEs were performed, and the results indicated that four FI-DEs (AC124854.1, LINC02609, U62317.1, and ZNF503-AS2) remained independently correlated with the OS of patients with KIRC (Figure 1B). The expression of AC124854.1, LINC02609, and U62317.1 was significantly increased, whereas the expression of ZNF503-AS2 was markedly decreased in patients with KIRC (Figure 1C). To clarify the expression of those four candidate prognostic biomarkers in KIRC, we selected other independent samples for verification. The expressions of AC124854.1, LINC02609, and ZNF503-AS2 in the ICGC dataset were consistent with that in the TCGA dataset (Figure 1D). There was no expression of U62317.1. Therefore, only the candidates AC124854.1, LINC02609, and ZNF503-AS2 were selected for the subsequent analyses. Patients with a high expression of LINC02609 displayed worse OS, while

patients with high expression of AC124854.1 and ZNF503-AS2 displayed better OS (Figures 1E–G).

3.2 Construction and validation of CIFI as a prognostic model

Based on previous studies, we constructed a risk assessment model using the three FI-DEs. The Youden index was used as the optimal cut-off value to regroup patients with KIRC (Supplementary Figure S3). The CIFI value and survival status of each patient with KIRC are shown in Figure 2A. In patients with KIRC having high CIFI values, the expression of LINC02609 was markedly increased, the expression of AC124854.1 was considerably decreased, and there was no substantial difference for ZNF503-AS2 (Figure 2B). Patients with KIRC and high CIFI values displayed a decreased OS (Figure 2C). Receiver operating characteristic (ROC) curve analyses indicated that the AUC value of this prognostic model was 0.75 (Figure 2D). Time-dependent ROC analyses

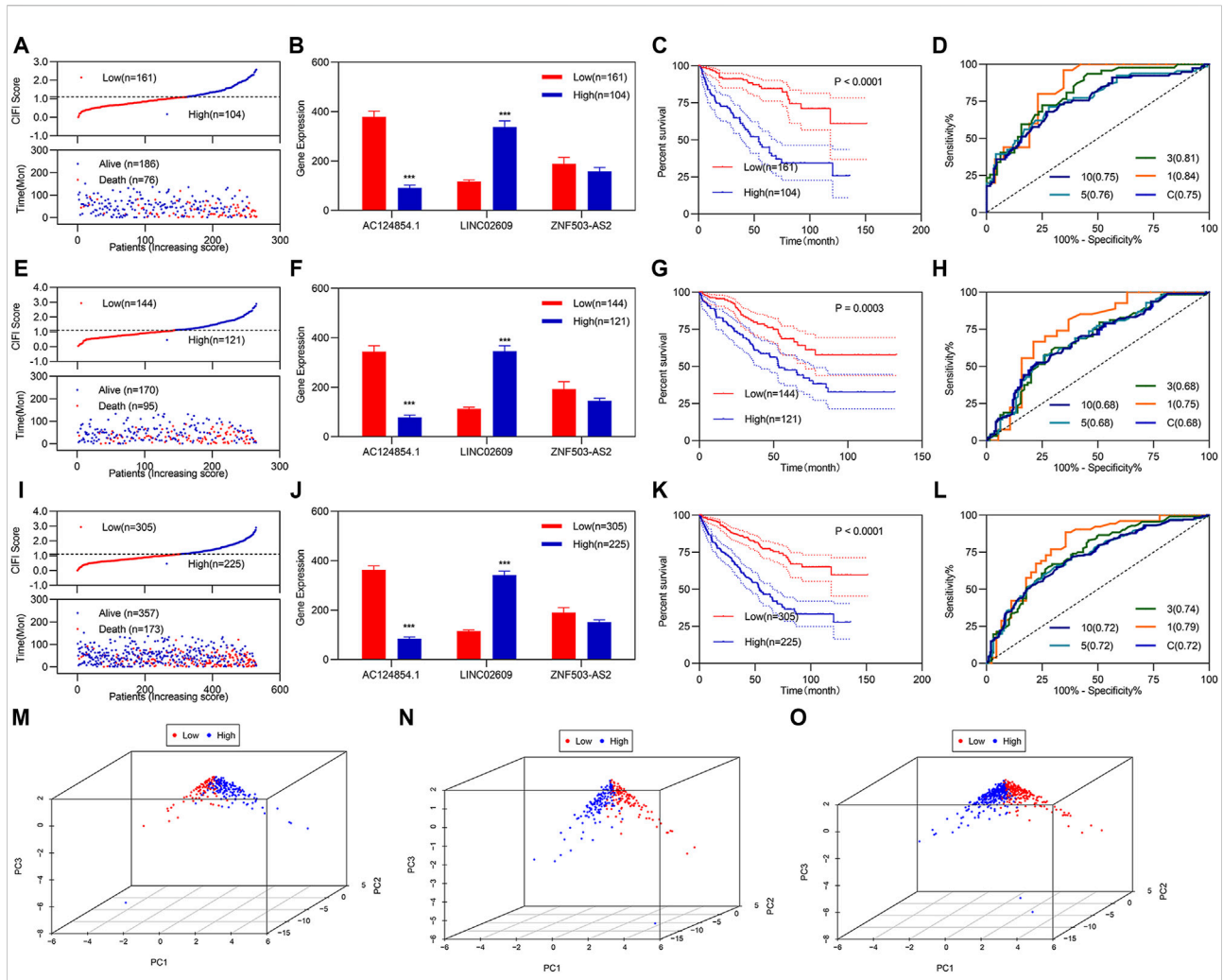


FIGURE 2 Development and validation of CIFI as a prognostic model. (A–D) and (M) Analysis of the prognostic model in the training group ($n = 265$). (A) For risk value (up) and survival status (down) for each patient. (B) Expression of the three candidate biomarkers. (C) K–M curve of KIRC patients with different CIFI values. (D) ROC curve of the risk assessment model. (M) Distribution of patients with different CIFI values. (E–H) and (N) Analysis of the prognostic model in the validation group ($n = 265$). (E) For risk value (up) and survival status (down) for each patient. (F) Expression of the three candidate biomarkers. (G) K–M curve of KIRC patients with different CIFI values. (H) ROC curve of the risk assessment model. (N) Distribution of patients with different CIFI values. i–l and o Analysis of the prognostic model in the entire group ($n = 530$). (I) For risk value (up) and survival status (down) for each patient. (J) Expression of the three candidate biomarkers. (K) K–M curve of KIRC patients with different CIFI values. (L) ROC curve of risk assessment model. (O) Distribution of patients with different CIFI values. * $p < 0.05$, ** $p < 0.01$, *** $p < 0.001$.

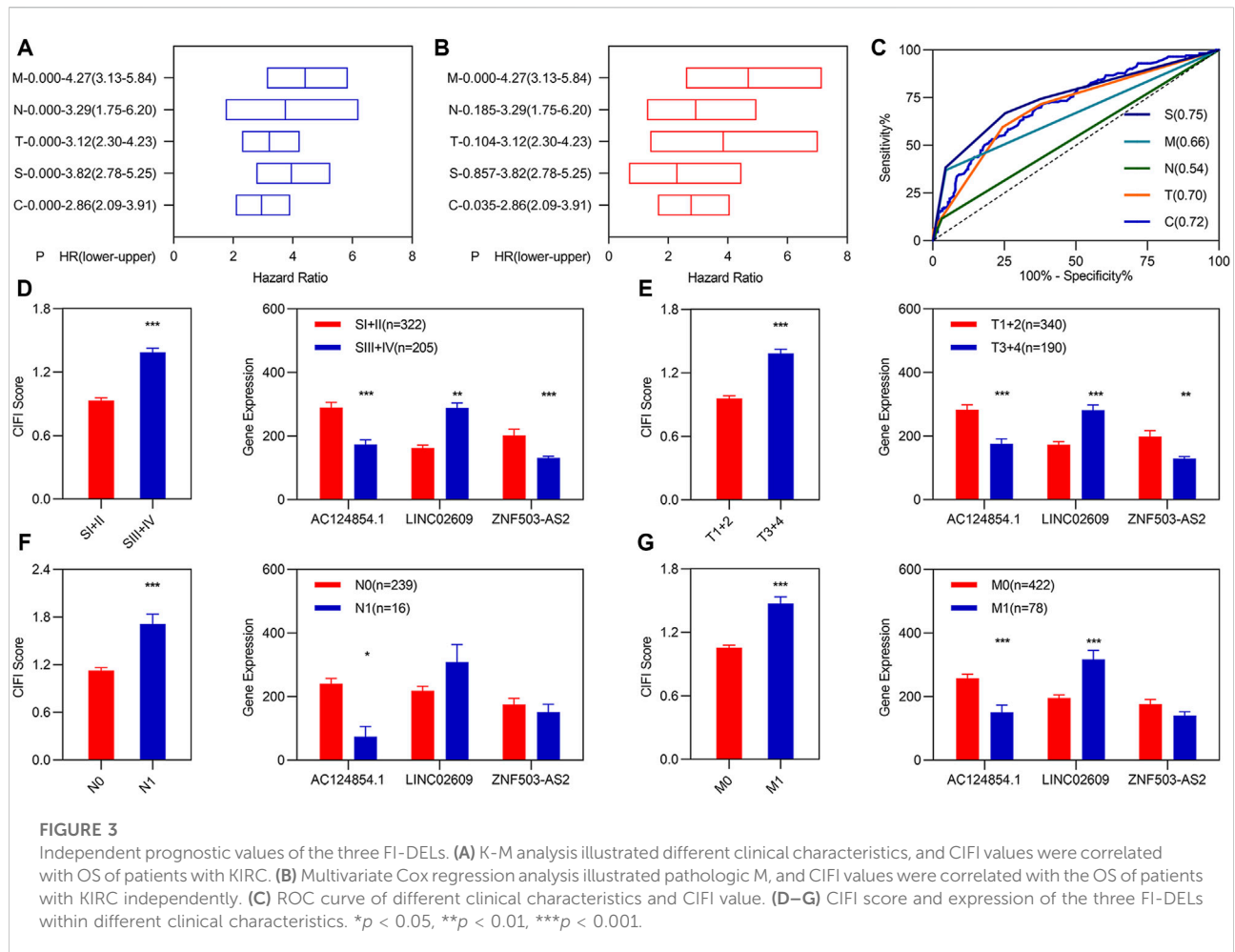
indicated that the AUC values at 1, 3, 5, and 10 years were 0.84, 0.81, 0.76, and 0.75, respectively (Figure 2D). Principal component analyses (PCA) showed that patients with different CIFI values could be well distinguished using the three FI-DEs (Figure 2M).

Verification regarding the three FI-DEs as feasible biomarkers was performed by validation studies in the validation and entire groups; which indicated similar results for the validation and entire groups (Figures 2E–L). Particularly, the AUC values were 0.68 and 0.72 in both the validation group and the entire group respectively (Figures 2H,L). PCA showed that patients with different CIFI values

could be well distinguished using the three FI-DEs in the validation and entire group (Figures 2N–O).

3.3 Independent prognostic model of the three ferroptosis- and immune-related differentially expressed lncRNAs

Previous studies have demonstrated that TNM classification and stage are usually used as predictors to assess the risk in patients with KIRC. To determine whether the CIFI score was an independent prognostic factor for patients with KIRC, we



performed univariate and multivariate Cox regression analyses among the clinical characteristics and CIFI scored in the entire group. Univariate Cox regression analyses showed that the CIFI score, pathologic TNM, and pathologic stage were significantly associated with the OS of KIRC (Figure 3A). Multivariate Cox regression analyses showed that the CIFI score and pathologic M were still significantly and independently associated with the OS of KIRC (Figure 3B). Subsequently, we plotted the ROC curve of the CIFI score and the different clinical characteristics and found that the AUC value of the CIFI score was higher than that of pathologic M (Figure 3C).

Correlation analyses showed that AC124854.1 and LINC02609 were significantly correlated with the CIFI values (Supplementary Figure S4). We carried out expression analyses to determine the relationship between the three FI-DEGs, CIFI scores, and clinical characteristics. The results are presented in Figures 3D–G. For example, the CIFI score was markedly associated with the pathologic TNM and stage (Figures 3D–G left). The expression of AC124854.1 was associated with the pathologic TNM, stage, and CIFI score (Figures 3D–G right).

3.4 Correlation analyses of CIFI with the immune cells and factors

After regrouping, we re-evaluated the stromal score, immune score, tumor purity, and ESTIMATE score between different clusters. There was no significant difference in stromal scores between patients with high and low CIFI values (Figure 4A). The immune and ESTIMATE scores were significantly increased, while tumor purity was significantly decreased in patients with KIRC with high CIFI values (Figures 4B–D). We performed correlation analyses for the estimated score with the three candidate biomarkers and CIFI values for patients with KIRC with high and low CIFI values (Figure 4E).

To determine which immune cells and immune factors were correlated with CIFI, differential expression analyses were first performed. There were 88 immune cells and immune factors that were markedly different between normal individuals and patients with KIRC (Supplementary Table S1). Of these, 56 immune cells and factors were considerably different between patients with KIRC with high and low CIFI values (Figures 4F–K). To further

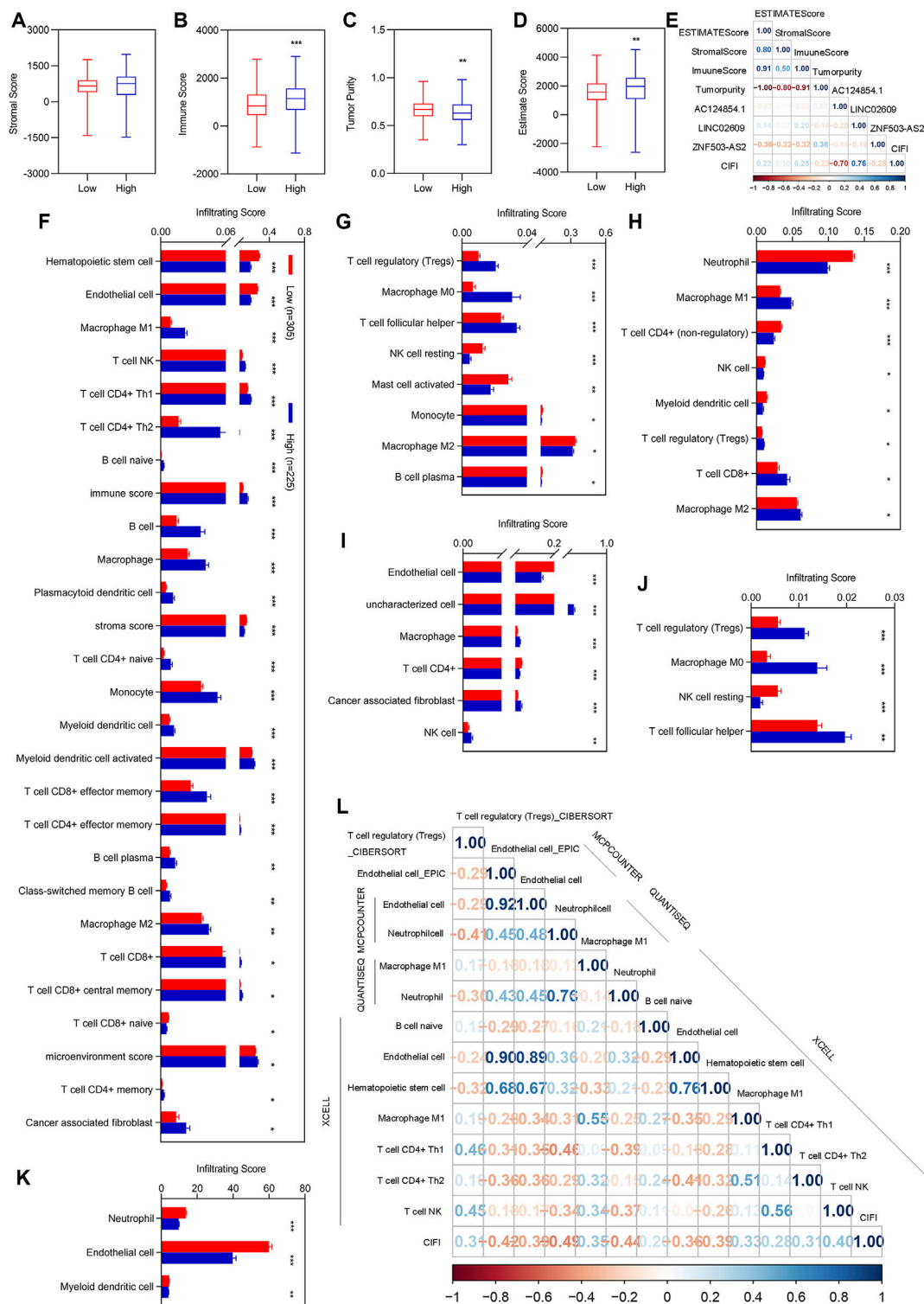


FIGURE 4

Correlation analysis of CIFI with the ESTIMATE score and immune infiltration. (A–D) Immune score between patients with KIRC with low CIFI value and patients with KIRC with high CIFI value. (A) Stromal score. (B) Immune score. (C) Tumor purity. (D) ESTIMATE score. (E) Correlation analysis of the three FI-DETs with the ESTIMATE Score. (F–K) Differentially expression analysis of the infiltrating score between patients with KIRC with low CIFI value and patients with KIRC with high CIFI value. (F) XCELL. (G) CIBERSORT. (H) quanTIseq. (I) EPIC. (J) CIBERSORT-ABS. (K) MCPCOUNTER. (L) Significantly associated immune cells and factors with CIFI. Correlation analysis of the prognostic model with the immune cells and factors. * $p < 0.05$, ** $p < 0.01$, *** $p < 0.001$.

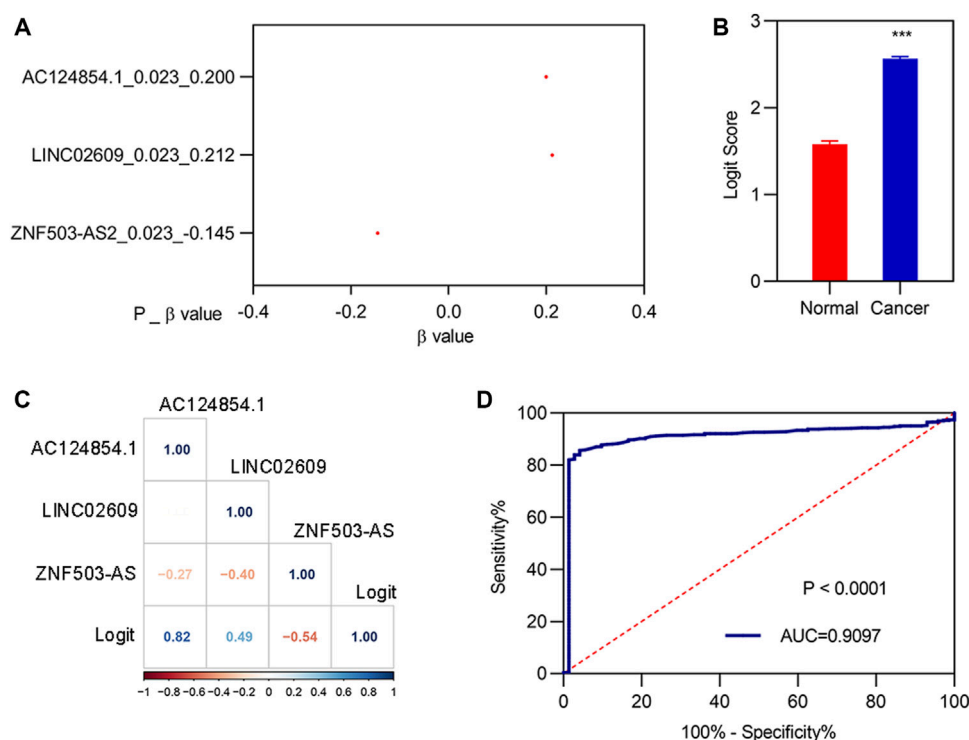


FIGURE 5

Construction of the diagnostic model. (A) β -value of the analysis of three FI-DEs by stepwise logistic regression. (B) Diagnosis values between normal and patients with KIRC. (C) Correlation analysis of the three FI-DEs with diagnosis values. (D) ROC curves of the diagnostic model. *** $p < 0.001$.

determine the relationship among these 56 immune cells and factors with CIFI values, Pearson correlation analyses were performed and 13 out of 56 immune cells and factors were correlated with the CIFI (Figure 4I).

3.5 Construction of logit (P) as a diagnostic model and enrichment analyses of Kyoto Encyclopedia of Genes and Genomes

To determine whether the three biomarkers could be used for the diagnosis of patients with KIRC, a diagnostic model was constructed and assessed. Stepwise logistic regression for the three FI-DEs (Figure 5A) was performed. The diagnosis score was markedly increased in patients with KIRC (Figure 5B) and was markedly correlated with AC124854.1, LINC02609, and ZNF503-AS2 (Figure 5C). The sensitivity and specificity of the diagnosis were 0.8566 and 0.9583, respectively (Table 2). The AUC value of this diagnostic model was 0.9097 (Figure 5D).

GSEA in R was used to compare the KEGG pathway between different clusters. We found that 60 signaling pathways were significantly enriched using the differentially expressed genes between normal and KIRC patients. The top 10 signaling

TABLE 2 Sensitivity and specificity of the diagnostic model.

	Real KIRC	Real normal
Predicted KIRC	454	3
Predicted normal	76	69
Total	530	72
Correct	454	69
Sensitivity	0.8566	
Specificity		0.9583

pathways are shown in Figures 6A–J. We found that only five signaling pathways were significantly enriched using the differentially expressed genes between low CIFI and high CIFI patients (Figure 6K–6O). However, the signaling pathways they enriched were quite different.

4 Discussion

Kidney cancer is a heterogeneous disease. KIRC is one of the most common subtypes of kidney cancer and is characterized by

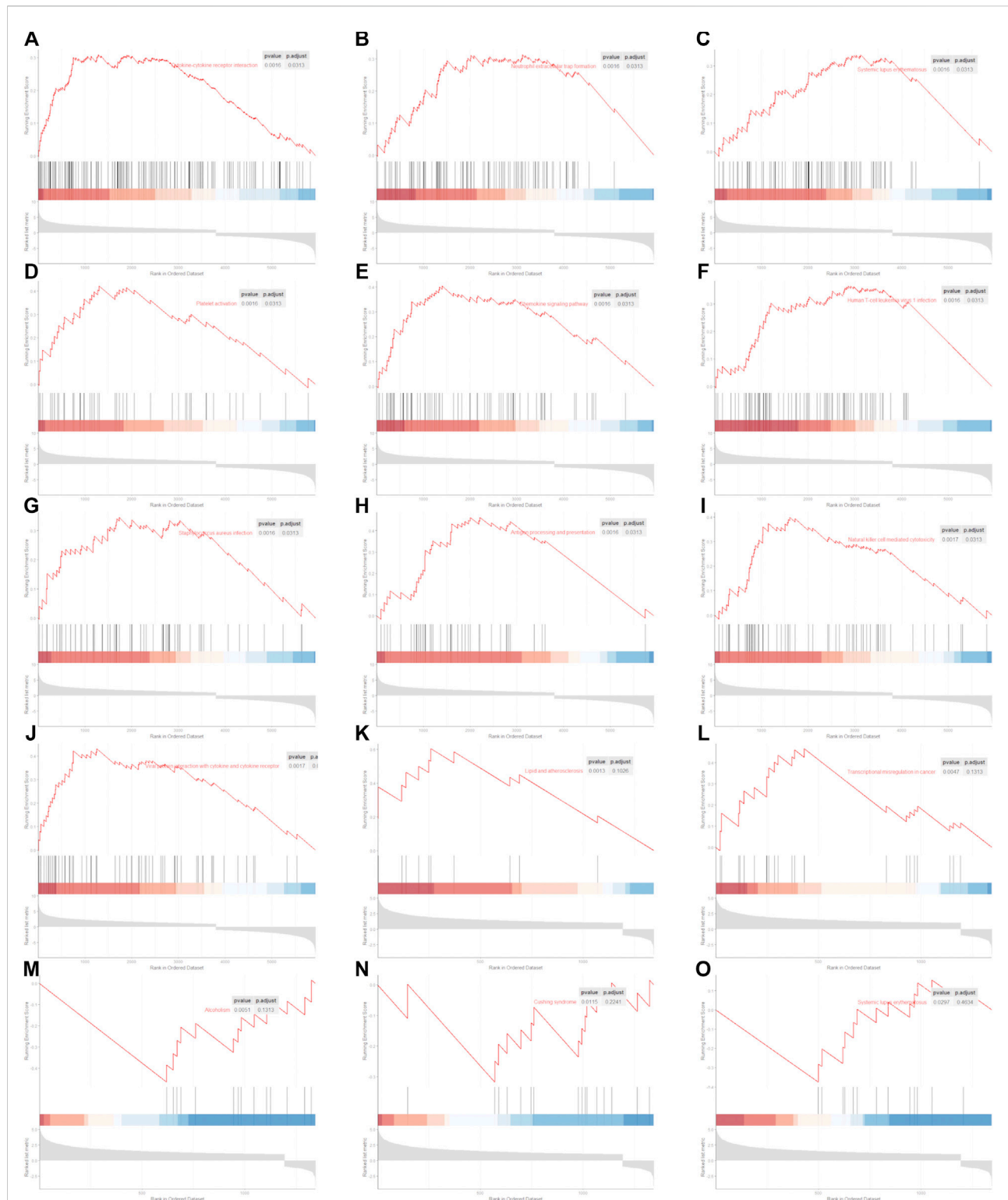


FIGURE 6

Significantly enriched KEGG pathway. (A–J) Top 10 significantly enriched signaling pathways between normal and KIRC. (A) Cytokine–cytokine receptor interaction. (B) Neutrophil extracellular trap formation. (C) Systemic lupus erythematosus. (D) Platelet activation. (E) Chemokine signaling pathway. (F) Human T-cell leukemia virus 1 infection. (G) *Staphylococcus aureus* infection. (H) Antigen processing and presentation. (I) Natural killer cell-mediated cytotoxicity. (J) Viral protein interaction with cytokine and cytokine receptor. (K–O) Five significantly enriched signaling pathways between patients with KIRC with low CIF value and patients with KIRC with high CIF value. (K) Lipid and atherosclerosis. (L) Transcriptional misregulation in cancer. (M) Alcoholism. (N) Cushing syndrome. (O) Systemic lupus erythematosus.

high morbidity, mortality, and poor prognosis worldwide (Zhao et al., 2018; Mendoza-Alvarez et al., 2019). Due to the limited biomarkers in prediction, some patients with KIRC may be diagnosed with inaccurate grades, which could influence their OS (Wang et al., 2019a). Therefore, identifying new suitable biomarkers with high sensitivity and specificity is crucial for the prognosis and diagnosis of KIRC.

In the current study, gene expression data and clinical information of KIRC were obtained from TCGA. We obtained 261 FI-DELS through differential expression and correlation analyses. For the 261 FI-DELS, we performed univariate Cox regression analyses, multivariate Cox regression analyses, and WGCNA and found that three FI-DELS could be used as biomarkers for patients with KIRC. We constructed prognostic and diagnostic models using the three FI-DELS. Univariate and multivariate Cox regression analyses indicated that the prognostic model using the three FI-DELS was an independent prognostic factor. In addition, we constructed a diagnostic model using the three FI-DELS. The AUC value of the diagnostic model was 0.9097, indicating that this diagnostic model may be feasible. Previous studies have indicated that the three biomarkers identified in the present study were related to OS in other cancers. For example, Wu et al. (2020) found that ZNF503-AS2 could be used as an independent prognostic biomarker for rhabdoid tumors of the kidney by univariate and multivariate Cox analyses. Xing et al. (2021) found that LINC02609 was associated with the OS of patients with KIRC. Cao et al. (2021) found that the glycolysis-related lncRNA AC124854.1 was markedly correlated with the OS of renal cancer by univariate and multivariate Cox regression analyses. Cheng et al. (2019) also found that AC124854.1 could be used as a prognostic and diagnostic biomarker for KIRC. Our results are consistent with those of previous studies that reinforced the feasibility of our results.

Previous studies have found that surgery is the primary treatment for patients with KIRC because most patients are resistant to radiation and chemotherapy (Zhao et al., 2018; Evelonn et al., 2019; Yin et al., 2019). Discovering recently, ferroptosis and immunity are new therapeutic targets for cancer. Additionally, some prognostic markers based on ferroptosis and immunity also exist. For example, the AUC value of the risk assessment model constructed by Sun et al. using immune-related lncRNA signatures was 0.71⁴⁵, and Xing et al. found that the AUC value of the risk assessment model constructed using the ferroptosis-related lncRNA signatures was 0.72⁴⁰. We compared the present prognostic lncRNA features with published predictive models in patients with KIRC. Yin et al. (2018) found that nine lncRNAs (SLC25A5-AS1, COL18A1-AS1, WT1-AS, AC016773.1, LINC00460, LINC00313, HOTTIP, FGF14-AS1, and AC10502.1) could serve as independent biomarkers to predict survival in patients with KIRC. Sun et al. (2020b) found five immune-related lncRNA signatures (AC008105.3, LINC02084, AC243960.1, AC093278.2,

and AC108449.2) with the ability to predict the prognosis of patients with KIRC. Liu et al. (2018) found that 19 lncRNAs (LOC606724, SCART1, SNORA8, LOC728024, HAVCR1P1, FCGR1CP, LINC00240, LINC00894, GK3P, SNHG3, KIAA0125, URB1-AS1, ZNF542P, TINCR, LINC00926, PDXDC2P, COL18A1-AS1, LINC00202-1, and LINC00937) that are potential biomarkers for the prognosis of KIRC. The AUC values of the three models were 0.684, 0.709, and 0.723, respectively, which were slightly lower than those of the present study (Liu et al., 2018; Yin et al., 2018; Sun et al., 2020b). Additionally, Zhang et al. (2019) found that 11 lncRNA signatures (AC245100.1, AP002761.1, LINC00488, AC017033.1, LINC-PINT, COL5A1-AS1, AC026471.4, AL009181.1, AL078590.3, LINC00524, and HOTTIP) could be potential biomarkers for KIRC. Yu et al. (2021) found that five prognostic-associated m6A-related lncRNAs (AC012170.2, AL157394.1, AP006621.2, AC025580.3, and AC124312.5) can be used as prognostic biomarkers for KIRC. The AUC values of these models were 0.781, and 0.809 respectively, which were slightly higher than those in the present study (Zhang et al., 2019; Yu et al., 2021). Comparatively, these two models used more prognostic biomarkers than those used in this study.

Although previous studies and our results indicate that the three FI-DELS may be used as prognostic and diagnostic biomarkers for patients with KIRC, the lack of cross-validation of other independent data and prospective clinical validation is an important shortcoming of our study. In addition, *in vitro* cell experiments and *in vivo* animal experiments are necessary to understand the functions of the three FI-DELS as biomarkers.

5 Conclusion

Through a series of bioinformatics analyses, we found that three FI-DELS (AC124854.1, LINC02609, and ZNF503-AS2) were independently significantly correlated with the OS of patients with KIRC. The prognostic and diagnostic models suggested that three FI-DELS could be used as prognostic and diagnostic biomarkers in patients with KIRC.

Data availability statement

Publicly available datasets were analyzed in this study. These data can be found at: <https://portal.gdc.cancer.gov/>.

Author contributions

ZH and HW conceived and designed the experiments; XX performed the analyses; YL helped in analyzing the data; and XX wrote the manuscript.

Conflict of interest

The authors declare that the research was conducted in the absence of any commercial or financial relationships that could be construed as a potential conflict of interest.

Publisher's note

All claims expressed in this article are solely those of the authors and do not necessarily represent those of their affiliated

organizations, or those of the publisher, the editors, and the reviewers. Any product that may be evaluated in this article, or claim that may be made by its manufacturer, is not guaranteed or endorsed by the publisher.

Supplementary material

The Supplementary Material for this article can be found online at: <https://www.frontiersin.org/articles/10.3389/fgene.2022.915372/full#supplementary-material>

References

- Berraondo, P., Minute, L., Ajona, D., Corrales, L., Melero, I., and Pio, R. (2016). Innate immune mediators in cancer: Between defense and resistance. *Immunol. Rev.* 274, 290–306. doi:10.1111/immr.12464
- Cao, H., Tong, H., Zhu, J., Xie, C., Qin, Z., Li, T., et al. (2021). A glycolysis-based long non-coding RNA signature accurately predicts prognosis in renal carcinoma patients. *Front. Genet.* 12, 638980. doi:10.3389/fgene.2021.638980
- Chaffer, C. L., and Weinberg, R. A. (2011). A perspective on cancer cell metastasis. *Science* 331, 1559–1564. doi:10.1126/science.1203543
- Chen, Y. P., Zhang, Y., Lv, J. W., Li, Y. Q., Wang, Y. Q., He, Q. M., et al. (2017). Genomic analysis of tumor microenvironment immune types across 14 solid cancer types: Immunotherapeutic implications. *Theranostics* 7, 3585–3594. doi:10.7150/thno.21471
- Cheng, G., Liu, D., Liang, H., Yang, H., Chen, K., and Zhang, X. (2019). A cluster of long non-coding RNAs exhibit diagnostic and prognostic values in renal cell carcinoma. *Aging (Albany NY)* 11, 9597–9615. doi:10.18632/aging.102407
- Dixon, S. J., Lemberg, K. M., Lamprecht, M. R., Skouta, R., Zaitsev, E. M., Gleason, C. E., et al. (2012). Ferroptosis: An iron-dependent form of nonapoptotic cell death. *Cell* 149, 1060–1072. doi:10.1016/j.cell.2012.03.042
- Efferth, T. (2017). From ancient herb to modern drug: Artemisia annua and artemisinin for cancer therapy. *Semin. Cancer Biol.* 46, 65–83. doi:10.1016/j.semcancer.2017.02.009
- Evelonn, E. A., Landfors, M., Haider, Z., Kohn, L., Ljungberg, B., Roos, G., et al. (2019). DNA methylation associates with survival in non-metastatic clear cell renal cell carcinoma. *BMC Cancer* 19, 65. doi:10.1186/s12885-019-5291-3
- Fazal, F. M., and Chang, H. Y. (2016). lncRNA structure: Message to the heart. *Mol. Cell* 64, 1–2. doi:10.1016/j.molcel.2016.09.030
- Forsea, A. M., Del Marmol, V., de Vries, E., Bailey, E. E., and Geller, A. C. (2012). Melanoma incidence and mortality in Europe: New estimates, persistent disparities. *Br. J. Dermatol.* 167, 1124–1130. doi:10.1111/j.1365-2133.2012.11125.x
- Im, A., and Pavletic, S. Z. (2017). Immunotherapy in hematologic malignancies: Past, present, and future. *J. Hematol. Oncol.* 10, 94. doi:10.1186/s13045-017-0453-8
- Johdi, N. A., and Sukor, N. F. (2020). Colorectal cancer immunotherapy: Options and strategies. *Front. Immunol.* 11, 1624. doi:10.3389/fimmu.2020.01624
- Kim, J., Piao, H. L., Kim, B. J., Yao, F., Han, Z., Wang, Y., et al. (2018). Long noncoding RNA MALAT1 suppresses breast cancer metastasis. *Nat. Genet.* 50, 1705–1715. doi:10.1038/s41588-018-0252-3
- Langfelder, P., and Horvath, S. (2008). Wgcna: an R package for weighted correlation network analysis. *BMC Bioinforma.* 9, 559. doi:10.1186/1471-2105-9-559
- Li, Z., and Rong, L. (2020). Cascade reaction-mediated efficient ferroptosis synergizes with immunomodulation for high-performance cancer therapy. *Biomater. Sci.* 8, 6272–6285. doi:10.1039/d0bm01168a
- Liu, T., Sui, J., Zhang, Y., Zhang, X. M., Wu, W. J., Yang, S., et al. (2018). Comprehensive analysis of a novel lncRNA profile reveals potential prognostic biomarkers in clear cell renal cell carcinoma. *Oncol. Rep.* 40, 1503–1514. doi:10.3892/or.2018.6540
- Liu, Y., Zhang, X., Zhang, J., Tan, J., Li, J., and Song, Z. (2020). Development and validation of a combined ferroptosis and immune prognostic classifier for hepatocellular carcinoma. *Front. Cell Dev. Biol.* 8, 596679. doi:10.3389/fcell.2020.596679
- Ljungberg, B., Bensalah, K., Canfield, S., Dabestani, S., Hofmann, F., Hora, M., et al. (2015). EAU guidelines on renal cell carcinoma: 2014 update. *Eur. Urol.* 67, 913–924. doi:10.1016/j.eururo.2015.01.005
- Mendoza-Alvarez, A., Guillen-Guio, B., Baez-Ortega, A., Hernandez-Perez, C., Lakhwani-Lakhwani, S., Maeso, M. D. C., et al. (2019). Whole-exome sequencing identifies somatic mutations associated with mortality in metastatic clear cell kidney carcinoma. *Front. Genet.* 10, 439. doi:10.3389/fgene.2019.00439
- Nie, J., Lin, B., Zhou, M., Wu, L., and Zheng, T. (2018). Role of ferroptosis in hepatocellular carcinoma. *J. Cancer Res. Clin. Oncol.* 144, 2329–2337. doi:10.1007/s00432-018-2740-3
- Nixon, N. A., BlaisN.ErnSt, S., Kollmannsberger, C., Bebb, G., ButlerM., et al. (2018). Current landscape of immunotherapy in the treatment of solid tumours, with future opportunities and challenges. *Curr. Oncol.* 25, e373–e384. doi:10.3747/co.25.3840
- Owens, B. (2016). Kidney cancer. *Nature* 537, S97. doi:10.1038/537S97a
- Salama, M. F., Carroll, B., Adada, M., Pulkoski-Gross, M., Hannun, Y. A., and Obeid, L. M. (2015). A novel role of sphingosine kinase-1 in the invasion and angiogenesis of VHL mutant clear cell renal cell carcinoma. *FASEB J.* 29, 2803–2813. doi:10.1096/fj.15-270413
- Shi, L., Liu, Y., Li, M., and Luo, Z. (2021). Emerging roles of ferroptosis in the tumor immune landscape: From danger signals to anti-tumor immunity. *FEBS J.* 289, 3655–3665. doi:10.1111/febs.16034
- Shibasaki, N., Yamasaki, T., Kanno, T., Arakaki, R., Sakamoto, H., Utsunomiya, N., et al. (2015). Role of IL13RA2 in sunitinib resistance in clear cell renal cell carcinoma. *PLoS One* 10, e0130980. doi:10.1371/journal.pone.0130980
- Singh, D. (2021). Current updates and future perspectives on the management of renal cell carcinoma. *Life Sci.* 264, 118632. doi:10.1016/j.lfs.2020.118632
- Slack, F. J., and Chinnaiyan, A. M. (2019). The role of non-coding RNAs in oncology. *Cell* 179, 1033–1055. doi:10.1016/j.cell.2019.10.017
- Song, J., Liu, Y. D., Su, J., Yuan, D., Sun, F., and Zhu, J. (2019). Systematic analysis of alternative splicing signature unveils prognostic predictor for kidney renal clear cell carcinoma. *J. Cell. Physiol.* 234, 22753–22764. doi:10.1002/jcp.28840
- Stockwell, B. R., and Jiang, X. (2019). A physiological function for ferroptosis in tumor suppression by the immune system. *Cell Metab.* 30, 14–15. doi:10.1016/j.cmet.2019.06.012
- Sun, J., Zhang, Z., Bao, S., Yan, C., Hou, P., Wu, N., et al. (2020). Identification of tumor immune infiltration-associated lncRNAs for improving prognosis and immunotherapy response of patients with non-small cell lung cancer. *J. Immunother. Cancer* 8, e000110. doi:10.1136/jitc-2019-000110
- Sun, Z., Jing, C., Xiao, C., and Li, T. (2020). Long non-coding RNA profile study identifies an immune-related lncRNA prognostic signature for kidney renal clear cell carcinoma. *Front. Oncol.* 10, 1430. doi:10.3389/fonc.2020.01430
- Sung, H., Ferlay, J., Siegel, R. L., Laversanne, M., Soerjomataram, I., Jemal, A., et al. (2021). Global cancer statistics 2020: GLOBOCAN estimates of incidence and mortality worldwide for 36 cancers in 185 countries. *Ca. Cancer J. Clin.* 71, 209–249. doi:10.3322/caac.21660
- Wang, D., Xie, N., Gao, W., Kang, R., and Tang, D. (2018). The ferroptosis inducer erastin promotes proliferation and differentiation in human peripheral blood mononuclear cells. *Biochem. Biophys. Res. Commun.* 503, 1689–1695. doi:10.1016/j.bbrc.2018.07.100

- Wang, Q., Zhang, H., Chen, Q., Wan, Z., Gao, X., and Qian, W. (2019). Identification of METTL14 in kidney renal clear cell carcinoma using bioinformatics analysis. *Dis. Markers* 2019, 5648783. doi:10.1155/2019/5648783
- Wang, W., Green, M., Choi, J. E., Gijon, M., Kennedy, P. D., Johnson, J. K., et al. (2019). CD8(+) T cells regulate tumour ferroptosis during cancer immunotherapy. *Nature* 569, 270–274. doi:10.1038/s41586-019-1170-y
- Wang, Z., Yang, B., Zhang, M., Guo, W., Wu, Z., Wang, Y., et al. (2018). lncRNA epigenetic landscape analysis identifies EPIC1 as an oncogenic lncRNA that interacts with MYC and promotes cell-cycle progression in cancer. *Cancer Cell* 33, 706–720. doi:10.1016/j.ccell.2018.03.006
- Wu, X., Liu, J., Zhu, C., Ma, M., Chen, X., Liu, Y., et al. (2020). Identification of potential biomarkers of prognosis-related long non-coding RNA (lncRNA) in pediatric rhabdoid tumor of the kidney based on ceRNA networks. *Med. Sci. Monit.* 26, e927725. doi:10.12659/MSM.927725
- Xie, L., Li, H., Zhang, L., Ma, X., Dang, Y., Guo, J., et al. (2020). Autophagy-related gene P4HB: A novel diagnosis and prognosis marker for kidney renal clear cell carcinoma. *Aging (Albany NY)* 12, 1828–1842. doi:10.18632/aging.102715
- Xing, X. L., Yao, Z. Y., Ou, J., Xing, C., and Li, F. (2021). Development and validation of ferroptosis-related lncRNAs prognosis signatures in kidney renal clear cell carcinoma. *Cancer Cell Int.* 21, 591. doi:10.1186/s12935-021-02284-1
- Yamaguchi, H., Hsu, J. L., Chen, C. T., Wang, Y. N., Hsu, M. C., Chang, S. S., et al. (2013). Caspase-independent cell death is involved in the negative effect of EGF receptor inhibitors on cisplatin in non-small cell lung cancer cells. *Clin. Cancer Res.* 19, 845–854. doi:10.1158/1078-0432.CCR-12-2621
- Yin, H., Wang, X., Zhang, X., Wang, Y., Zeng, Y., Xiong, Y., et al. (2018). Integrated analysis of long noncoding RNA associated-competing endogenous RNA as prognostic biomarkers in clear cell renal carcinoma. *Cancer Sci.* 109, 3336–3349. doi:10.1111/cas.13778
- Yin, L., Li, W., Wang, G., Shi, H., Wang, K., Yang, H., et al. (2019). NR1B2 suppress kidney renal clear cell carcinoma (KIRC) progression by regulation of LATS 1/2-YAP signaling. *J. Exp. Clin. Cancer Res.* 38, 343. doi:10.1186/s13046-019-1344-3
- Yu, J., Mao, W., Sun, S., Hu, Q., Wang, C., Xu, Z., et al. (2021). Identification of an m6A-related lncRNA signature for predicting the prognosis in patients with kidney renal clear cell carcinoma. *Front. Oncol.* 11, 663263. doi:10.3389/fonc.2021.663263
- Zhang, E., He, X., Zhang, C., Su, J., Lu, X., Si, X., et al. (2018). A novel long noncoding RNA HOXC-AS3 mediates tumorigenesis of gastric cancer by binding to YBX1. *Genome Biol.* 19, 154. doi:10.1186/s13059-018-1523-0
- Zhang, J., Zhang, X., Piao, C., Bi, J., Zhang, Z., Li, Z., et al. (2019). A long non-coding RNA signature to improve prognostic prediction in clear cell renal cell carcinoma. *Biomed. Pharmacother.* 118, 109079. doi:10.1016/j.biopha.2019.109079
- Zhang, Z., Yan, C., Li, K., Bao, S., Li, L., Chen, L., et al. (2021). Pan-cancer characterization of lncRNA modifiers of immune microenvironment reveals clinically distinct de novo tumor subtypes. *NPJ Genom. Med.* 6, 52. doi:10.1038/s41525-021-00215-7
- Zhao, H., Cao, Y., Wang, Y., Zhang, L., Chen, C., Wang, Y., et al. (2018). Dynamic prognostic model for kidney renal clear cell carcinoma (KIRC) patients by combining clinical and genetic information. *Sci. Rep.* 8, 17613. doi:10.1038/s41598-018-35981-5
- Zhou, J., Zhu, Y., Liu, Y., Niu, P., Chen, H., Deng, J., et al. (2020). High PRAS40 mRNA expression and its role in prognosis of clear cell renal cell carcinoma. *Transl. Androl. Urol.* 9, 1650–1660. doi:10.21037/tau-20-741
- Zhou, M., Zhang, Z., Bao, S., Hou, P., Yan, C., Su, J., et al. (2021). Computational recognition of lncRNA signature of tumor-infiltrating B lymphocytes with potential implications in prognosis and immunotherapy of bladder cancer. *Brief. Bioinform.* 22, bbaa047. doi:10.1093/bib/bbaa047